Supplemental Document

Biomedical Optics EXPRESS

Visual inertial odometry enabled 3D ultrasound and photoacoustic imaging: supplement

DEEKSHA M. SANKEPALLE,[1] BRIAN ANTHONY,[2] AND SRIVALLEESHA MALLIDI[1,3,*]

[1] *Department of Biomedical Engineering, Tufts University, Medford, MA, 02155, USA*
[2] *Institute of Medical Engineering and Sciences, Department of Mechanical Engineering, Massachusetts Institute of Technology, Cambridge, MA, 02139, USA*
[3] *Wellman Center for Photomedicine, Harvard Medical School, Boston, MA, 02115, USA*
[*] *Srivalleesha.mallidi@tufts.edu*

Supplement DOI: https://doi.org/10.6084/m9.figshare.22716442

Parent Article DOI: https://doi.org/10.1364/BOE.489614

Visual Inertial Odometry enabled 3D Ultrasound and Photoacoustic imaging: Supplemental document

DEEKSHA M SANKEPALLE,[1] BRIAN ANTHONY,[2] AND SRIVALLEESHA MALLIDI[1,3,*]

[1]Department of Biomedical Engineering, Tufts University, Medford, MA, USA 02155
[2]Institute of Medical Engineering and Sciences, Department of Mechanical Engineering, Massachusetts Institute of Technology, Cambridge, MA, USA 02139
[3]Wellman Center for Photomedicine, Harvard Medical School, Boston, MA, USA 02115
**Srivalleesha.mallidi@tufts.edu*

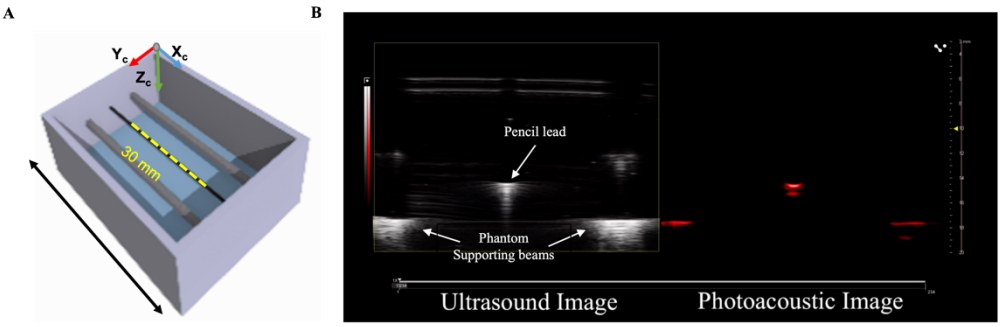

Fig. S1: **A)** Representation of the phantom with a 0.7 mm pencil lead (black) in between two supporting beams (grey) used for USPAI imaging, black arrow depicts the direction of motion and yellow dashed line is the length of lead imaged. **B)** Snapshot of **Visualization S1** which contains USPA images of the pencil lead (point source) acquired over time during forward and backward motion of the integrated probe.

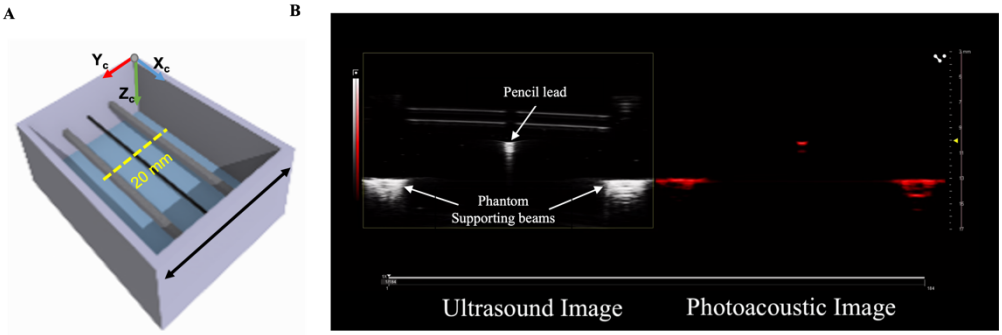

Fig. S2: **A)** Representation of the phantom with a 0.7 mm pencil lead (black) in between two supporting beams (grey) used for USPAI imaging, black arrow depicts the direction of motion and yellow dashed line is the length of lead imaged. **B)** Snapshot of **Visualization S2** which contains USPA images of the pencil lead (point source) acquired over time during left and right motion of the integrated probe.

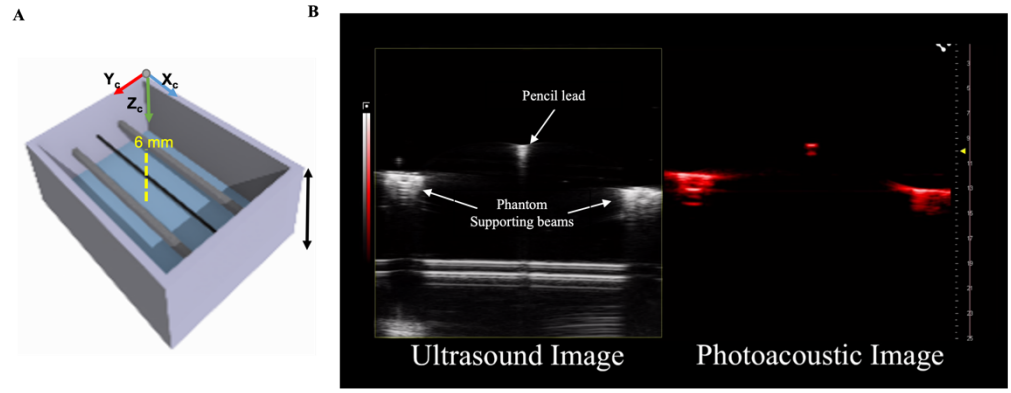

Fig. S3: **A)** Representation of the phantom with a 0.7 mm pencil lead (black) in between two supporting beams (grey) used for USPAI imaging, black arrow depicts the direction of motion and yellow dashed line is the length of lead imaged. **B)** Snapshot of **Visualization S3** which contains USPA images of the pencil lead (point source) acquired over time during up and down motion of the integrated probe.

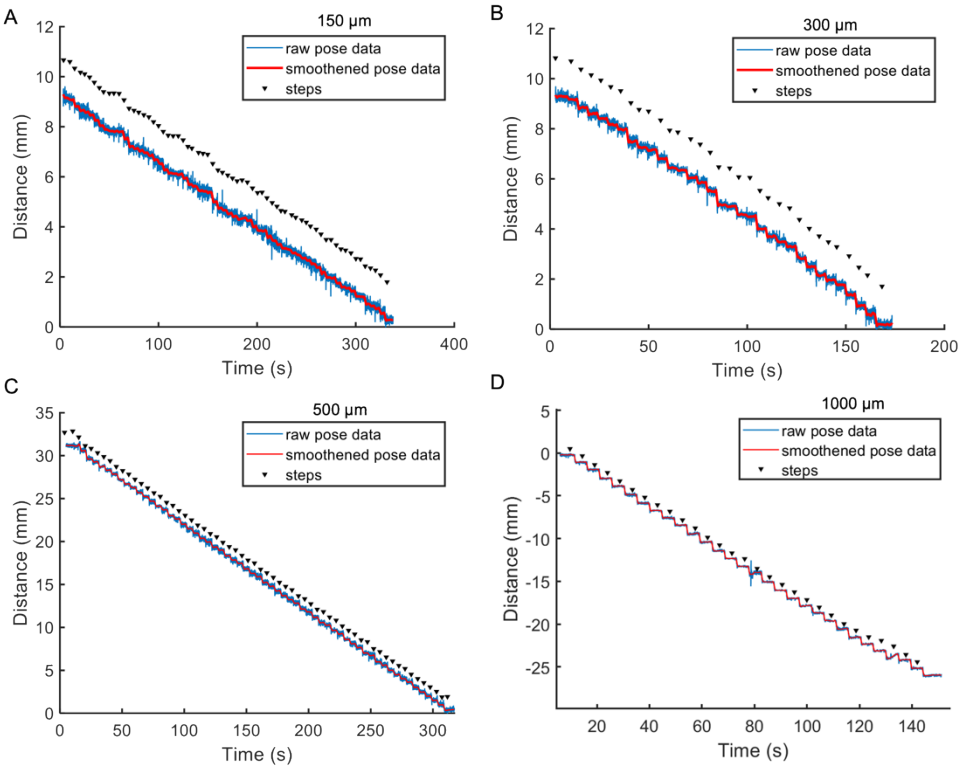

Fig. S4: Plot of raw pose data acquired for data presented in Fig. 4. Raw pose data is shown in blue line, Savitzky-Golay smoothened pose data overlaid as red line and the number of steps identified by a custom MATLAB code with the findpeaks command are shown as black triangular markers. **A)** Total of 67 steps for 150 µm step-size over a range of 10 mm. **B)** Total of 34 steps for 300 µm step-size over a range of 100 mm. **C)** Total of 62 steps for 500 µm step-size over a range of 300 mm. **D)** Total of 30 steps for 1000 µm step-size over a range of 300 mm.

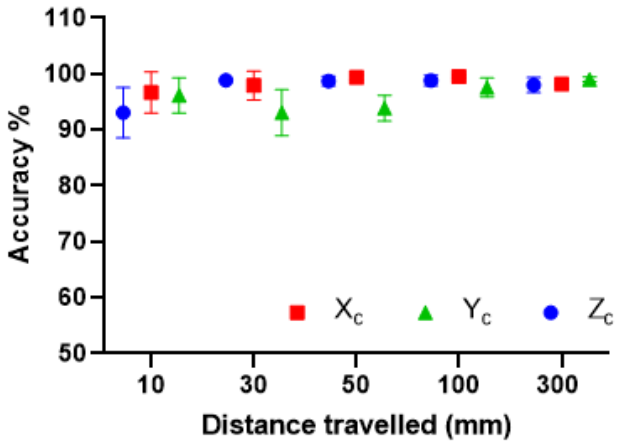

Fig. S5: Accuracy of the camera pose data for various distance travelled (10-300 mm range) along different axis.

Table S1: Accuracy and repeatability of the camera pose data compared to distance programmed on a linear stage for various distances travelled at 1, 5 and 10 mm/s speed along all three axes (n=3 measurements for each row).

Distance on linear stage (mm)	Speed (mm/s)	Distance measured on camera (mm)	Error (mm)	Accuracy (%)	Repeatability (mm)
X_c Axis					
10	1	9.9479	0.052	98.21	0.1162
	5	9.9624	0.037	97.59	
	10	9.7542	0.245	94.21	
30	1	29.4256	0.574	97.89	0.1020
	5	29.6295	0.370	98.26	
	10	29.5344	0.465	97.57	
50	1	49.7599	0.240	99.51	0.1018
	5	49.8755	0.124	99.34	
	10	49.9627	0.037	99.26	
100	1	99.9834	0.016	99.56	0.1513
	5	99.7234	0.276	99.49	
	10	99.9875	0.012	99.65	
300	1	295.2327	4.767	98.41	0.5794
	5	294.1789	5.821	98.05	
	10	294.2882	5.711	98.09	
Average accuracy (%)				98.33 %	
Average repeatability (mm)					0.2101

Y_c Axis					
10	1	10.2097	0.209	95.50	0.0217
	5	10.2349	0.234	96.84	
	10	10.2530	0.253	96.21	
30	1	32.0486	2.048	93.17	0.0691
	5	32.1574	2.157	92.80	
	10	32.0291	2.029	93.23	
50	1	53.1066	3.106	93.78	0.0533
	5	53.0007	3.000	93.99	
	10	53.0630	3.063	93.87	
100	1	102.4583	2.458	97.54	0.1293
	5	102.5530	2.553	97.44	
	10	102.2972	2.297	97.72	
300	1	302.9770	2.977	99.00	0.1241
	5	303.0416	3.041	98.98	
	10	302.8018	2.801	99.06	
Average accuracy (%)				95.94 %	
Average repeatability (mm)					0.0795
Z_c Axis					
10	1	10.7809	0.780	92.19	0.1120
	5	10.5673	0.567	94.32	
	10	10.7323	0.732	92.67	
30	1	29.8633	0.136	98.56	0.1062
	5	29.8807	0.119	99.08	
	10	30.0554	0.055	98.92	
50	1	49.2158	0.784	98.43	0.1343
	5	49.4391	0.560	98.87	
	10	49.4569	0.543	98.86	
100	1	98.7965	1.203	98.79	0.1332
	5	98.6858	1.314	98.68	
	10	98.9510	1.049	98.95	
300	1	292.7644	7.235	97.58	1.8014
	5	293.2443	6.755	97.74	
	10	296.0966	3.903	98.69	
Average accuracy (%)				97.49 %	
Average repeatability (mm)					0.4574